

## **Review**

### **Vibrational spectroscopy and its future applications in microbiology**

#### **Authors:**

Miia M Jansson (corresponding author)

miia.jansson@oulu.fi

Adjunct professor (PhD), senior researcher

Research Unit of Medical Imaging, Physics and Technology, University of Oulu, Oulu, Finland

ORCID: 0000-0001-5815-0325

Martin Kögler

martin.kogler@vtt.fi

Senior scientist (PhD), sensing solutions at VTT – Technical Research Centre of Finland, Oulu, Finland

ORCID: 0000-0003-2154-8879

Sohvi Hörkkö

sohvi.horkko@oulu.fi

Professor (MD, PhD)

Research Unit of Biomedicine, Medical Microbiology and Immunology, Faculty of Medicine, University of Oulu, Oulu, Finland

ORCID: 0000-0003-2118-5270

Tero Ala-Kokko

tero.ala-kokko@ppshp.fi

Professor (MD, PhD)

Division of Intensive Care, Department of Anesthesiology, Oulu University Hospital, Oulu, Finland

Research Group of Surgery, Anesthesiology and Intensive Care, Medical Research Center Oulu, Oulu, Finland

ORCID: 0000-0001-8841-2701

Lassi Rieppo

lassi.rieppo@oulu.fi

Adjunct professor (PhD), senior researcher

Research Unit of Medical Imaging, Physics and Technology, University of Oulu, Oulu, Finland

ORCID: 0000-0001-5542-406

## **ABSTRACT**

Vibrational spectroscopic techniques, namely Fourier transform infrared (FTIR) and Raman spectroscopy, are based on the study of molecular vibrations, and they are complementary techniques to each other. This review provides an overview of the vibrational spectroscopic techniques applied in microbiology during the past decade. In addition, future applications of the elaborated spectroscopic techniques will be highlighted. The results of this review show that both FTIR and Raman spectroscopy are promising alternatives to conventional diagnostic approaches because they provide label-free and non-invasive bacterial detection, identification, and antibiotic susceptibility testing in a single step. Cost-effective, accurate, and rapid tests are needed in order to improve diagnostics and patient care, to decrease the use of unnecessary antimicrobial agents, to prevent resistant microbials, and to decrease the overall burden of outbreaks. Prior to that, however, the presented approaches need to be validated in a clinical workflow against the conventional diagnostic approaches.

**Keywords:** Fourier transform infrared spectroscopy, Microbiology, Raman spectroscopy, Time-gated Raman spectroscopy, Surface-enhanced Raman spectroscopy

## Introduction

The conventional diagnostic approaches (e.g., immunology-based approaches, nucleic acid identification, spectrometry-based procedures, i.e., mass spectrometry) have relied on phenotypic and genetic markers to identify an infection according to species or strain, antimicrobial susceptibility, virulence, and/or metabolic characteristics.<sup>[1, 2]</sup> These approaches, however, are time consuming and frequently expensive,<sup>[1, 3]</sup> increasing the likelihood of physicians prescribing empirical antimicrobial therapies instead of tailored, pathogen-directed therapy.<sup>[1]</sup> In addition, the obtained results can be culture negative due to previously administered antimicrobials. Misuse and overuse of antimicrobials are accelerating the development and spread of antimicrobial resistance (AMR).

Inappropriate antimicrobial use and the treatment of antimicrobial-resistant infections have a major economic burden for health care.<sup>[4-6]</sup> Furthermore, the overuse of antimicrobials leads to mortality due to antimicrobial-resistant health care-associated infections.<sup>[7]</sup> A recent report on the casualties related to AMR estimated that about 700,000 people die annually on global level due to drug-resistant diseases.<sup>[8]</sup> If no action is taken, drug-resistant diseases could cause 10 million deaths globally each year by 2050, ensuring that AMR would be the most prevalent cause of death.<sup>[8]</sup> For that reason, a large deal of work has been done to develop alternative methods for fast bacterial identification in suspected patients.<sup>[9]</sup>

Different biomolecules are characterized by unique molecular compositions, leading to subtle differences in their corresponding vibrational spectra. Within the last decades, optical detection of biomolecules has been used extensively in various fields (e.g., health, pharmacy, safety, food) for the identification of the chemical composition and molecular structure of different substances and microorganisms.<sup>[10-12]</sup> Biological isolates are very complex as even a single cell or a bacterium is composed of several biomolecules, such as proteins, lipids, carbohydrates, and nucleic acids. Therefore, these spectral markers can be used to identify pathogens and biological processes. Furthermore, chemometric analysis can be used to increase the discrimination ability of these techniques and it provides the possibility for quantitative analysis.

In this paper, multidisciplinary databases were reviewed to provide an overview of the vibrational spectroscopic techniques applied in microbiology during the past decade. In addition, future applications of the elaborated techniques will be highlighted, with a focus on clinical isolates. Due to the high versatility of the vibrational spectroscopic techniques, the review integrates its various diagnostic powers into an applied discussion targeted at the needs of clinicians and medical microbiologists.

## **An overview of vibrational spectroscopy in microbiology**

Vibrational spectroscopic techniques, namely Fourier transform infrared (FTIR) and Raman spectroscopy, are based on the study of molecular vibrations, and they are complementary techniques to each other. FTIR spectroscopy is a chemical analytical technique that generates the absorbance spectra of molecules in the infrared region of the electromagnetic spectrum of a molecule. Correspondingly, Raman spectroscopy is a label-free optical technology based on the inelastic scattering of light. FTIR spectra provide a unique spectro-chemical signature that is related to the molecular vibrations (see Fig. 1). Respectively, the wavelength shifts in Raman scattering are molecule specific and can be displayed as a Raman spectrum (see Fig. 2). Since different microorganisms will differ in their biochemical composition (e.g., their nucleic acids, polysaccharides, proteins), this will be reflected in their spectra, enabling the accurate epidemiological characterization of those microorganisms (see Fig. 3).

These techniques present several advantages in the field of clinical, industrial, and environmental microbiology: vibrational spectroscopy provides label-free bacterial detection, identification, and antimicrobial susceptibility testing (AST) in a single step, performed directly on a sample (e.g., a solid, liquid, or semi-solid) without staining and labeling. Furthermore, FTIR and Raman spectroscopy allow performing real-time measurements non-invasively in continuous mode without the necessity of invasive sampling or sample preparation.<sup>[11]</sup> In general, these techniques are fast, accurate, and sensitive, but their potential is not yet fully utilized in clinical microbiology.

### ***Vibrational spectroscopy in microbial typing***

FTIR spectroscopy has a great potential for the identification of both taxonomically close species of the same genus and taxonomically distant species of a different genus (see Table 1).<sup>[13-14]</sup> Recently, for instance, Guliev et al. identified *Staphylococcus aureus* (*S. aureus*) among both taxonomically close and distant species from a comprehensive set of control strains by creating a classification model that is independent of the media and culture growth stage.<sup>[13]</sup> A similar study was conducted by Lasch et al., who identified eight taxonomically distinct Gram-positive and Gram-negative strains from three different sample sets by using FTIR hyperspectral imaging in combination with an artificial neural network (ANN)-based image segmentation.<sup>[14]</sup> In addition, reduced cultivation time was used to overcome constraints related to spectral contamination.

Bacterial identification contributes to the epidemiologic surveillance of epidemic clones of the same species (e.g., strains and serotypes).<sup>[15-18]</sup> According to Nyarko et al., FTIR spectroscopy is a highly discriminatory and reproducible method that can be used for the rapid typing of live and dead populations of organisms.<sup>[15]</sup> The authors showed that the epidemic clones of *Listeria monocytogenes* (J1-101, J1-129, J1-220, R2-499), as well as viable and heat-killed

populations of the bacteria, can be differentiated from clinical and food isolates by using FTIR spectroscopy and multivariate statistical analysis (chemometrics). A similar study was conducted by Grunert et al.<sup>[17]</sup> who used ANN-assisted FTIR spectroscopy to overcome constraints related to conventional serotyping by discriminating epidemic clones of *S. aureus* from different origins and control strains via metabolic fingerprinting. According to the authors, FTIR spectroscopy coupled to chemometric analysis was found to be an interesting tool, not only for clinical diagnostics but also for understanding the mechanisms of bacterial adaptation.

### ***Vibrational spectroscopy in bacterial infections***

Urinary tract infections (UTIs) are the most common type of health care-associated infection reported to the National Healthcare Safety Network.<sup>[19]</sup> Although urine culture is the gold standard for the diagnosis of UTI, it is relatively expensive and time consuming, requiring at least 24–48 hours to produce results. In addition, the diagnostic accuracy of dipstick tests has remained low.<sup>[20]</sup> Recently, however, vibrational spectroscopic techniques have been found to be a rapid alternative to UTI diagnosis.<sup>[21-23]</sup>

In the study of AlRabiah et al., for instance, the discrimination ability of FTIR spectroscopy was found to be similar to a virulence test but not with metabolic test.<sup>[21]</sup> In the other study, clinically relevant concentrations ( $10^2$ – $10^4$  CFU/ml) of bacterial volatile organ compounds (VOCs) were discriminated from human blood and urine via a SERS substrate and a portable Raman spectrometer (see Table 3).<sup>[22]</sup> With this, a point-of-care-amenable method was found to be a promising alternative to the conventional gas-sensing technologies used to detect bacteria-derived VOCs directly from a urine sample. In the third study, Raman spectrometry was combined with dielectrophoresis to capture the structure and composition of *Escherichia coli* and *Enterococcus faecalis* from dilute suspensions.<sup>[23]</sup> In addition, fused silica was used as a chip substrate to get high-quality Raman spectra. According to the authors, a robust classification model can be built with the help of multivariate statistical analysis.<sup>[23]</sup>

Blood culture remains the most widespread technique for bloodstream infections, but unfortunately it requires 12–24 hours.<sup>[24]</sup> Although the integration of nucleic acid-based methods has significantly reduced the response time, it has not eliminated the need for additional culture.<sup>[24]</sup> In the study of Pazos-Perez et al.,<sup>[25]</sup> clinically relevant Gram-positive and Gram-negative strains were detected and quantified in low concentrations in real time and in a multiplexed manner by using a microorganism optical detection system (MODS) in conjunction with SERS-labeled silver (Ag) nanoparticles (NPs). According to authors, a SERS-enhanced MODS analysis has the potential to be used in the culture-free identification of several bloodstream pathogens (e.g., viruses, protozoa, fungus, and neoplastic cells) from complex body fluids within minutes.

SERS-active substrates can also be used for the rapid and accurate detection of lower respiratory tract infections.<sup>[26-28]</sup> In the study of Rivera-Betancourt et al., for instance, Ag nanorods were prepared by an oblique-angle deposition technique and fabricated by using a custom-designed electron-beam/sputtering evaporation system.<sup>[26]</sup> A total of nine *Mycobacterium* strains belonging to four species were analyzed in conjunction with chemometric techniques based on the SERS spectra of the mycolic acids of the mycobacterial cell envelope.<sup>[26]</sup> Correspondingly, the clinically relevant concentration of the *Mycoplasma pneumoniae* strain (M129) was separated from respiratory secretions by using Ag nanorod array (NA)-based SERS in conjunction with a quantitative polymerase chain reaction (qPCR).<sup>[27]</sup> With this, NA-SERS was found to be an equal alternative to the qPCR, which highlights the potential usage of NA-SERS in point-of-care testing (POCT).<sup>[27]</sup>

So far, the biomedical applications of spectroscopic gas sensing technologies have been limited.<sup>[29, 30]</sup> In the study of Choi et al., however, a continuous optofluidic SERS platform was used in conjunction with standard polystyrene-latex particles to detect airborne particles in real time.<sup>[29]</sup> Prior to that, an optical sensor element with two-dimensional correlation analysis was used to detect bacterial VOCs in the low-ppm range from complex VOC mixtures.<sup>[30]</sup> According to the authors, a significantly higher sensitivity (even on a ppb range) can be obtained via wave optics than can be obtained from the nanostructured sensors required for conventional SERS.

### ***Vibrational spectroscopy in AST***

AST is a critical part of microbial typing and medical decision-making: it confirms susceptibility, detects resistance, and guides the selection of antimicrobials in clinical practice. AST may be done by using a variety of techniques (e.g., disk diffusion, gradient diffusion, and agar/broth dilution), which are sensitive and easy to use, but yield a non-quantitative classification of antimicrobial susceptibility (e.g., susceptible, intermediate, or resistant). Since the late 1980s, epsilometer testing (Etest) has been used to determine the minimum inhibitory concentrations (MICs) of antimicrobial agents against bacteria. Etest is, however, time consuming (16–24 h) and laborious in a daily practice.<sup>[31]</sup> In addition, antimicrobial disks are not always available for new drugs.<sup>[32]</sup> Novel methods for fast, reliable, and cost-effective screening tools for AST are urgently warranted.

Vibrational spectroscopy has been found to be a suitable alternative for AST.<sup>[33-42]</sup> Rodrigues et al., for instance, assessed the potential and robustness of FTIR spectroscopy in antimicrobial genotyping by combining molecular genotypic, comparative genomics, and biochemical data in multivariate analyses.<sup>[33]</sup> Antibiotic susceptibility was also tested by Bauer et al., who used Raman spectroscopy in conjunction with Etest.<sup>[41]</sup> Taken together, a Raman-based AST

assay demonstrated good correlation in comparison to Etest, but reduced the total analysis time to 3.5 hours, which is at least 25% less time-consuming than conventional methods.

Recent studies have also shown the enormous potential of Raman spectroscopy in rapid MIC determination.<sup>[35, 37-38, 41]</sup> In the study of Liu et al., for instance, a SERS-based approach was used in conjunction with Ag NPs and the standard broth dilution method for bacterial AST and MIC determination.<sup>[36]</sup> The results obtained were in good agreement with the ones obtained with the traditional methods and no major error was found according to the Clinical and Laboratory Standards Institute's guidelines.

### ***Vibrational spectroscopy in fungal infections***

According to the Centers for Disease Control and Prevention, there were over 75,000 hospitalizations and nearly 9 million outpatient visits for fungal diseases in the USA in 2017.<sup>[43]</sup> Although the most common cause of candidiasis is *Candida albicans* (*C. albicans*), the emergence of *Candida dubliniensis*, *Candida glabrata*, *Candida krusei*, *Candida parapsilosis* (*C. parapsilosis*), and *Candida tropicalis* has increased over the past decades,<sup>[44]</sup> and *Candida auris* has recently been recognized as a globally emerging multidrug-resistant species.<sup>[45, 46]</sup> Conventional methods (e.g., microscopy, selective culture, and/or biochemical approaches) used in the identification of yeast pathogens and their drug-resistance profiles lack satisfactory sensitivity and specificity, and often require prior culturing of the infecting agent.<sup>[47]</sup> For that reason, there is a growing interest in the development of alternative methods, based on the direct detection of diagnostic molecules.<sup>[48-50, 53-54]</sup>

In the study of Wohlmeister et al., three *Candida* species and seven reference strains were discriminated from vaginal isolates, and the colonies were phenotypically identified using a Perkin Elmer's FTIR/FT-NIR spectrometer in conjunction with CHROMagar™ *Candida*.<sup>[48]</sup> Correspondingly, Colabella et al.<sup>[49]</sup> extracted four pathogenic *Candida* species from blood by using a FTIR spectrometer in conjunction with DNA barcoding. In the study of Potocki et al., three *Candida* species and three reference strains (e.g., haploid, diploid, tetraploid strains) were characterized in terms of their karyotype patterns, DNA content, and biochemical features by using FTIR in conjunction with Raman spectroscopy.<sup>[50]</sup> With this, spectra-based molecular fingerprinting was found to be a promising alternative to karyotype profiling and DNA content analysis, reflecting the genomic diversity of clinical isolates. The authors also postulated that Raman spectroscopy can provide information to be used in antifungal susceptibility testing. According to the authors, however, the lack of FTIR spectral libraries is the major limitation in the FTIR-based identification of *Candida* strains,<sup>[49-50]</sup> which is in line with bacterial strains.<sup>[13-14, 51-52]</sup>

## ***Vibrational spectroscopy in viral infections***

Viral infections are currently identified by detecting circulating antibodies, viral antigens, or by a nucleic acid amplification test. In the study of Ditta et al., however, the viral load of hepatitis C was identified using a PeakSeeker spectrometer from the plasma of both infected and healthy individuals using 60 mW of laser light (785 nm) in the region of 1,800–600  $\text{cm}^{-1}$  for 30 s.<sup>[55]</sup> According to the authors, Raman spectroscopy can be used in conjunction with principal component analysis to identify the biochemical changes during hepatitis C virus infection.

More recently, viruses have been identified from clinical isolates using low-cost, paper-based SERS or carbon nanotube assays, and microfluidics with handheld Raman devices or miniaturized mobile phone add-on spectrometer setups. This was recently demonstrated on rhino, influenza, and parainfluenza viruses,<sup>[56]</sup> as well as dengue viruses,<sup>[57]</sup> and human immunodeficiency viruses,<sup>[58]</sup> with sufficient accuracy. Since the outbreak of the coronavirus disease 2019 (COVID-19), Raman spectroscopy has also been utilized for the detection of the COVID-19 infection with high accuracy, precision, sensitivity, and specificity. In the study of Carlomagno, for instance, a current or past COVID-19 infection was detected by using Raman spectroscopy in conjunction with an rRT-PCR procedure from dried saliva drops.<sup>[59]</sup> The sample preparation processing and analytical procedures were simplified in order to obtain clinically relevant concentrations in a specific SERS regimen within a few minutes.

## **The advantages and disadvantages of vibrational spectroscopy in microbiology**

FTIR spectroscopy provides a highly specific whole-organism fingerprint and presents a highly discriminatory and reproducible method for real-time surveillance and outbreak analysis due to its label-free and unambiguous identification of molecular species within minutes (see Table 2).<sup>[14-18, 33, 48-49, 60]</sup> In fact, the discriminatory power of FTIR spectroscopy has been shown to be comparable to whole-genome sequencing, which is considered as the gold standard in genotyping.<sup>[33, 60]</sup> In addition, it has been more favorable in terms of accessibility and cost than the latest molecular genetic methods.<sup>[2, 13-14, 16-18]</sup> Because this method can be nondestructive and non-perturbative, FTIR spectroscopy can also be used to understand the diversity, evolution, and host adaptation of pathogens, and to monitor the biochemical changes occurring in a sample over time.<sup>[2, 33]</sup>

Systematic cultivation and imaging protocols are needed to enhance the reproducibility,<sup>[2, 13-14]</sup> whereas the discriminatory power can be improved by using supervised learning methods for spectrum analysis.<sup>[13-14, 17-18]</sup> In addition, further testing with a diverse sample is needed to enhance discrimination capabilities.<sup>[13, 17]</sup> The advantages and disadvantages of different spectra acquisition methods with varying sample preparation methods should also be

considered<sup>[2]</sup>; different techniques have small variations in peak intensity and position due to the amount of reflected radiation.

In microbial typing, attenuated total reflectance (ATR)<sup>[21, 33-34, 49, 60]</sup> and transmission<sup>[13-14, 16-17, 21, 48]</sup> spectroscopy have been the most commonly used techniques, followed by a diffuse-reflection method.<sup>[49]</sup> ATR is a simple, convenient, and reliable method; it is low-cost, highly reproducible, and nondestructive, making it suitable for metabolomic analysis, as an example.<sup>[2]</sup> Correspondingly, the transmission technique offers high quality spectra with a wide variety of spectral libraries available. However, ATR spectroscopy is simpler and quicker than the transmission mode due to the minor sample preparation procedures: both solid and liquid samples can be directly loaded onto the internal reflection element (IRE) crystal without major incubation requirements.<sup>[2]</sup> In addition, it is more resistant to water and air bubble interference.

Raman spectroscopy provides information regarding the presence, concentration, and chemical composition, with high selectivity due to the unique spectral fingerprint of each molecule. In addition, Raman spectroscopy has been shown to be a sensitive and a much faster alternative to conventional assays for antimicrobial and antifungal suitability testing (see Table 4).<sup>[23, 35-36, 41-42, 50]</sup> In line with FTIR spectroscopy, Raman spectroscopy can also be used to monitor the biochemical changes occurring in a sample over time.<sup>[25, 30, 42, 81]</sup> Compared with FTIR spectra, however, Raman spectra have sharper features, enabling higher selectivity, and are more resistant to water interference.<sup>[30, 61]</sup> In the future, however, further testing with a diverse sample is needed to increase discrimination capability. In line with ATR spectroscopy, a spectral library of well-characterized microbial species and strains is also needed to enhance reproducibility.

Both FTIR and Raman spectra contain a multitude of spectral information whereas spectral pre- and post-processing can be used to minimize the influence of irrelevant information (e.g., ambient light, thermal emissions). Conventional continuous wave excitation Raman spectroscopy, for instance, is insensitive to the typically low concentrations of bacterial and fungal signals and often suffers from strongly interfering background fluorescence. For that reason, several approaches have been developed to overcome the interference of fluorescent background, for example, shifted-excitation Raman difference spectroscopy, coherent anti-Stokes Raman spectroscopy, resonance Raman spectroscopy, and time-gated (TG) Raman spectroscopy.<sup>[62]</sup> In addition, the influence of auto-fluorescence has been minimized by using SERS. The use of TG-SERS diminishes the interference of background fluorescence from the biomolecules in the bacteria and the culture media.<sup>[63]</sup>

In microbial typing, aluminum slide and Ag NPs have been used to boost the Raman signal.<sup>[22, 25, 27, 29, 36, 54-55]</sup> Silver and gold NPs allow for million-fold signal enhancement and can be used for direct or indirect detection (SERS tags). Under some circumstances, non-toxic Au NPs can be used for intracellular *in vivo* detection (see Fig. 3).<sup>[64-65]</sup> It should be noted, however, that Raman spectra and SERS have different sensitivities to different parts of the cell. Raman spectra

detect a signal from throughout the illuminated sample volume, while in SERS, the enhancement is dependent on the distance from the NP or nanostructures, and molecules in the cell wall tend to be preferentially detected. For Raman spectroscopy, this is due to the number density of scattering molecules near the cytoplasm of the cell, whereas for SERS, the enhancement mechanism is distance dependent in the sub-nanometer range and NPs or structures pick up the signal more from the cell wall.<sup>[66]</sup>

## Discussion

This systematic review of 42 published studies investigated the work that has been carried out in the field of microbiology using FTIR and Raman spectroscopy. The results of this review show that both FTIR and Raman spectroscopy are promising alternatives to conventional diagnostic approaches because they provide label-free and non-invasive bacterial detection, identification, antimicrobial and antifungal susceptibility testing, and biofilm characterization in a single step. Prior to that, however, the presented approaches need to be validated in a clinical workflow against the conventional diagnostic approaches with diverse samples to get closer to the diagnostic requirements.

An ideal diagnostic test would be objective, inexpensive, and clinically available at the bedside, enabling rapid exclusion of the presence of bacterial infection and, thus, withholding certain patients from receiving antimicrobials unnecessarily. Recent achievements in nanoscience, spectroscopy, magnetism,<sup>[67]</sup> plasmonics,<sup>[68]</sup> and microfluidics<sup>[56]</sup> have created tremendous opportunities for clinical monitoring and diagnostics, particularly with the use of NPs and microparticles.<sup>[61]</sup> Both FTIR and Raman spectroscopy provide fast and accurate methods for real-time specie, serotype, and strain levels, antimicrobial susceptibility and virulence testing, and biofilm characterization in an accurate and a cost-effective way. In fact, vibrational spectroscopy has been found to be an equal alternative to conventional diagnostic approaches with high sensitivity and specificity, and the costs have been more than 30% lower than the competing methods<sup>[33, 60, 69]</sup> without significant maintenance or operating costs.<sup>[9, 17]</sup> Due to its remarkable sensitivity, vibrational spectroscopy can reduce mortality, the severity of clinical infection, the length of hospital stay, and the associated costs relative to conventional time-consuming culture-based techniques: clinically relevant concentrations of the microbes of can be detected within hours from clinical isolates.<sup>[22, 25, 27, 29]</sup> Indeed, the suspended cultures of clinical isolates can be directly analyzed on an optically dense crystal by using ATR-FTIR spectroscopy, for instance.<sup>[2]</sup> In literature, daily diagnostic testing with novel diagnostic approaches has been found to reduce in-patient mortality, resulting in an incremental cost-effectiveness ratio per life-year saved.<sup>[70]</sup> Improved microbiological diagnostics and subsequent improvements in clinical decision-making lead to a decreased risk of unnecessary antibiotic treatment as well as. This, on

the other hand, has significant economic consequences in addition to a decreased risk of the evolution of microbial resistance to drugs.

The use of vibrational spectroscopic techniques has presented several advantages in microbiology, which will potentially lead to new clinical bedside applications in the near future. In the context of real-time surveillance, as well as outbreak analyses, both FTIR and Raman spectroscopy have found to be valuable and easy-to-use alternatives to conventional diagnostic approaches (e.g., pulsed-field gel electrophoresis, whole-genome sequencing, multilocus sequence typing), which are often limited to retrospective studies. In addition, Raman spectroscopy has been found to be an equal alternative to molecular-based methodologies (e.g., PCR, qPCR, rRT-PCR), which also highlights the potential usage of NA-SERS in POCT,<sup>[27]</sup> the need for which has been accelerated by COVID-19. Indeed, a significant increase in the utilization of Raman spectroscopy can be seen in recent years,<sup>[59, 75]</sup> whereas the cost of the bench Raman instrument has been reduced by using a portable version.<sup>[59]</sup> In summary, the main reason for using Raman and/or FTIR spectroscopy is the possibility that these techniques can be used as real-time analytical tools that often lack traditional diagnostic approaches. In the future, however, additional efforts in research and development are needed; of course, real-time analytics depends on reliable software algorithms. In addition, clinical validation and commercial viability assessment are warranted.<sup>[1]</sup>

FTIR and Raman spectroscopy are often combined with confocal microscopes to improve spatial accuracy. However, such high accuracy is not always beneficial, especially when a temporal change needs to be monitored. Depending on the probing system, portable process spectroscopic devices—even with a fluorescence-suppressing TG option for Raman—are suitable for the analysis of microbiological isolates.<sup>[56-58]</sup> Their larger focal spot size allows for more repeatable results with enhancement methods (e.g., SERS; surface-enhanced infrared absorption spectroscopy [SEIRAS]). Several handheld, portable vibrational spectroscopic devices (e.g., Mira, Misa, Smart Raman XI™, BRAVO, Cora100, ASSURX, VIRRION) are already on the market that enable the easy use of SERS in conjunction with suitable commercially available substrates. Properly used, these enhancement methods can diminish the influence of disturbing background signals while amplifying the signals of specimens at the detection spot and to an affordable level.

Forthcoming approaches need to be used in a clinical workflow against the conventional diagnostic approaches. In the study of Martak et al., for instance, FTIR spectroscopy was applied to the daily work of a clinical laboratory.<sup>[16]</sup> Epidemic clones of Gram-negative bacilli infections were discriminated from control strains using a Bruker's IR Biotyper, an FTIR spectrometer designed to discriminate isolates by exploring the differences of the surface cell polysaccharides. During the clinical trial, the FTIR spectroscopy was found to be an accurate and faster alternative to conventional diagnostic approaches. In addition, reduced cultivation time and adequate spectral preprocessing and analysis strategies

should be used to improve reproducibility and robustness.<sup>[14]</sup> In addition, several spectrum replicates for each sample need to be taken to enhance reproducibility.<sup>[17, 48-49]</sup> A spectral library of well-characterized microbial species or strains is required to enhance reproducibility. Healthcare provider and scientific companies (e.g., Thermo Fisher Scientific, Wiley) are providing these spectral libraries, which might be beneficial if software algorithms compare the actual measurements with the features in the spectral databases. Spectroscopic gas sensing technologies are fast, non-destructive, long-term stable, and highly selective.<sup>[71-72]</sup> So far, however, the biomedical applications of spectroscopic gas sensing technologies have been limited as the low molecule density in gases results in a weak signal. In addition, sample collection from exhaled human breath has been labor intensive and difficult, requiring the usage of non-disposable materials such as sensors, mass flow controllers, Tedlar bags, glass syringes, and suction tubes.<sup>[73]</sup> Previously, a wide range of breath sample analysis methods (e.g., gas chromatography, proton transfer reactions, a selected ion flow tube, ion mobility-based spectrometry, secondary electrospray ionization) and laser spectroscopic techniques (e.g., tunable diode laser absorption; cavity ringdown-, integrated cavity output-, cavity enhanced absorption-, cavity leak-out-, photoacoustic-, quartz-enhanced photoacoustic-, and optical frequency comb cavity-enhanced absorption spectroscopy) have been used to detect targeted and nontargeted VOCs and/or volatile metabolites.<sup>[72, 74]</sup> These technologies, however, have required bulky instruments, complex sampling methods, and qualified personnel, which has limited their application in POCT. Alternatively, some electronic noses (e.g., Cyranose 320, DiagNose, BreathSpec, ChemPro100i) and colorimetric methods have been developed for POCT, but they have suffered from laborious pretreatment, low sensitivity, and being incapable of detecting unknown targets.

Future studies should focus on the identification of both viral and multidrug-resistant *Candida* species; viral pandemics (e.g., influenza A, Ebola), as well as antifungal resistance, are presenting a serious threat to global health today.<sup>[76-77]</sup> In addition, there is a clinical need for the rapid and accurate identification of pathogens directly from peripheral blood, which has been hampered due to the low concentration of organisms circulating in blood.<sup>[78]</sup> Vibrational spectroscopic techniques could also be applied in the analysis of cerebrospinal fluid. In literature, SEIRAS has overcome the limitations related to traditional FTIR spectroscopy<sup>[68, 79]</sup> but SEIRAS has not been applied to clinical isolates. In addition, breath VOC analysis for detecting infection requires further research and development; no current VOC biomarkers of infection have been clinically approved as yet.<sup>[74]</sup> For that reason, the sample collection for gas analysis needs to be simplified. Some of these techniques can also be fully automated in the near future by AI/software.

## Conclusion

The need for new diagnostic approaches is urgent in order to improve diagnostics and patient care, and to decrease the overall burden of AMR. Future technologies (e.g., vibrational spectroscopy, imaging-based technologies, electronic

noses, nuclear magnetic resonance, flow cytometry assays) are promising alternatives for bacterial identification and antibiotic profiling.<sup>[1]</sup> In fact, future technologies are expected to revolutionize the field of clinical diagnostics and thus the prevention and management of infectious diseases. In the future, bacterial identification and antibiotic profiling should be done in a second-to-minute timeframe. In addition, future technologies should eliminate cultivation restrictions and allow the virtually immediate prescription of the most adequate antibiotic therapy. In addition, the miniaturization of sensing devices should be conducted to promote the development of portable and battery-operated IoT devices to be used in POCT. Rapid diagnostics can also create new business models and thus redesign the care processes. Prior to that, however, the presented approaches need to be validated in a clinical workflow against the conventional diagnostic approaches to get closer to the diagnostic requirements. In addition, a spectral library of well-characterized microbial species and strains is required to identify unknown isolates.

### **Acknowledgements**

We acknowledge clinical microbiologist Maria-Teresa Martin-Gomez, who served as another clinical advisor.

### **Disclosure statement**

The authors declare they have no conflict of interest.

### **Funding**

None.

## References

- [1] Maugeri, G.; Lychko, I.; Sobral, R.; Roque, A. C. A. Identification and Antibiotic-Susceptibility Profiling of Infectious Bacterial Agents: A Review of Current and Future Trends. *Biotechnol J* 2019, 14, e1700750. doi:10.1002/biot.201700750.
- [2] Chirman, D; Pleshko, N. Characterization of bacterial biofilm infections with Fourier transform infrared spectroscopy: a review. *Appl Spectrosc Rev.* 2021. doi:10.1080/05704928.2020.1864392.
- [3] Váradi, L.; Luo, J. L.; Hibbs, D. E.; Perry, J. D.; Anderson, R. J.; Orenga, S.; Groundwater, P. W. Methods for the detection and identification of pathogenic bacteria: past, present, and future. *Chem Soc Rev.* 2017, 46, 818–4832. doi:10.1039/c6cs00693k.
- [4] Thorpe, K. E.; Joski, P.; Johnston, K.J. Antibiotic-Resistant Infection Treatment Costs Have Doubled Since 2002, Now Exceeding \$2 Billion Annually. *Health Aff.* 2018, 37, 662–669. doi: 10.1377/hlthaff.2017.1153.
- [5] Dadgostar, P. Antimicrobial Resistance: Implications and Costs. *Infect Drug Resist.* 2019,12,3903–3910. doi:10.2147/IDR.S234610.
- [6] Touat, M.; Opatowski, M.; Brun-Buisson, C.; Cosker, K.; Guillemot, D.; Salomon, J.; Tuppin, P.; de Lagasnerie, G.; Watier, L. A Payer Perspective of the Hospital Inpatient Additional Care Costs of Antimicrobial Resistance in France: A Matched Case-Control Study. *Appl Health Econ Health Policy* 2019, 17, 381–389. doi:10.1007/s40258-018-0451-1.
- [7] Touat, M.; Brun-Buisson, C.; Opatowski, M.; Salomon, J.; Guillemot, D.; Tuppin, P.; de Lagasnerie, G.; Watier, L. Costs and Outcomes of 1-year post-discharge care trajectories of patients admitted with infection due to antibiotic-resistant bacteria. *J Infect.* 2021, 82, 339–345. doi:10.1016/j.jinf.2021.02.001.
- [8] Interagency Coordination Group of antimicrobial resistance. No time to wait: Securing the future from drug-resistant infections. Report to the secretary-general of the United Nations. <https://www.who.int/antimicrobial-resistance/interagency-coordination-group/final-report/en/> (accessed April 21, 2021).
- [9] Novais, Â.; Freitas, A. R.; Rodrigues, C; Peixe, L. Fourier transform infrared spectroscopy: unlocking fundamentals and prospects for bacterial strain typing. *Eur J Clin Microbiol Infect Dis.* 2019, 38, 427–448. doi:10.1007/s10096-018-3431-3.
- [10] Rohman, A.; Anjar, W.; Endang, L.; Betania, K.; Fadzillah, N. A. The Use of FTIR and Raman Spectroscopy in Combination with Chemometrics for Analysis of Biomolecules in Biomedical Fluids: A Review. *Biomed Spectro Imag.* 2019, 8, 55–71. doi:10.3233/BSI-200189.

- [11] Kögler, M.; Zhang, B.; Cui, L.; Shi, Y.; Yliperttula, M.; Laaksonen, T.; Viitala, T.; Zhang, K. Real-time Raman based approach for identification of biofouling. *Sens Act B: Chemical* 2016; 230: 411–421. doi:10.1016/j.snb.2016.02.0790925-4005.
- [12] Naumann, D.; Helm, D.; Labischinski, H. Microbiological characterizations by FT-IR spectroscopy. *Nature* 1991, 351, 81. doi:10.1038/351081a0.
- [13] Guliev, R. R.; Suntsova, A. Y.; Vostrikova, T. Y.; Shchegolikhin, A. N.; Popov, D. A.; Guseva, M. A.; Shevelev, A. B.; Kurochkin, I. N. Discrimination of *Staphylococcus aureus* Strains from Coagulase-Negative Staphylococci and Other Pathogens by Fourier Transform Infrared Spectroscopy. *Anal Chem.* 2020, 92, 4943–4948. doi:10.1021/acs.analchem.9b05050.
- [14] Lasch, P.; Stämmler, M.; Zhang, M.; Baranska, M.; Bosch, A.; Majzner, K. *Anal. Chem.* 2018, 90, 8896–8904. doi:10.1021/acs.analchem.8b01024.
- [15] Nyarko, E. B.; Puzey, K. A.; Donnelly, C. W. Rapid Differentiation of *Listeria monocytogenes* Epidemic Clones III and IV and Their Intact Compared with Heat-Killed Populations Using Fourier Transform Infrared Spectroscopy and Chemometrics. *J Food Science* 2014, 79, M1189–M1193. doi:10.1111/1750-3841.12475.
- [16] Martak, D.; Valot, B.; Sauget, M.; Cholley, P.; Thouverez, M.; Bertrand, X.; Hocquet, D. Fourier-Transform InfraRed Spectroscopy Can Quickly Type Gram-Negative Bacilli Responsible for Hospital Outbreaks. *Front Microbiol.* 2019, 26, 1440. doi:10.3389/fmicb.2019.01440.
- [17] Grunert, T.; Wenning, M.; Barbagelata, M. S.; Fricker, M.; Sordelli, D. O.; Buzzola, F. R.; Ehling-Schulz, M. Rapid and reliable identification of *Staphylococcus aureus* capsular serotypes by means of artificial neural network-assisted Fourier transform infrared spectroscopy. *J Clin Microbiol.* 2013, 51, 2261–2266. doi:10.1128/JCM.00581-13.
- [18] Vogt, S.; Löffler, K.; Dinkelacker, A. G.; Bader, B.; Autenrieth, I. B.; Peter, S.; Liese, J. Fourier-Transform Infrared (FTIR) Spectroscopy for Typing of Clinical *Enterobacter cloacae* Complex Isolates. *Front Microbiol.* 2019, 10, 2582. doi:10.3389/fmicb.2019.02582.
- [19] National Healthcare Safety Network. Current HAI Progress Report. <https://www.cdc.gov/nhsn/datastat/index.html> (accessed April 21, 2021).
- [20] Mambatta, A. K.; Jayarajan, J.; Rashme, V. L.; Harini, S.; Menon, S.; Kuppusamy, J. Reliability of dipstick assay in predicting urinary tract infection. *J Family Med Prim Care* 2015, 4, 265–268. doi:10.4103/2249-4863.154672.

- [21] AlRabiah, H.; Xu, Y.; Rattray, N. J.; Vaughan, A. A.; Gibreel, T.; Sayqal, A.; Upton, M.; Allwood, J. W.; Goodacre, R. Multiple metabolomics of uropathogenic *E. coli* reveal different information content in terms of metabolic potential compared to virulence factors. *Analyst* 2015, 139, 4193. doi: 10.1039/c4an00176a.
- [22] DeJong, C. S.; Wang, D. I.; Polyakov, A.; Rogacs, A.; Simske, S. J.; Shkolnikov, V. Bacterial detection and differentiation via direct volatile organic compound sensing with surface enhanced raman spectroscopy. *Chemistryselect* 2017, 2, 8431–8435. doi:10.1002/slct.201701669.
- [23] Schröder, U.C.; Ramoji, A.; Glaser, U.; Sachse, S.; Leiterer, C.; Csaki, A.; Hübner, U.; Fritzsche, W.; Pfister, W.; Bauer, M.; Popp, J.; Neugebauer, U. Combined dielectrophoresis-Raman setup for the classification of pathogens recovered from the urinary tract. *Anal Chem.* 2013, 85, 10717–10724. doi: 10.1021/ac4021616.
- [24] Opota O.; Croxatto A.; Prod'hom G.; Greub G. Blood culture-based diagnosis of bacteraemia: state of the art. *Clin Microbiol Infect.* 2015, 21, 313–322. doi:10.1016/j.cmi.2015.01.003.
- [25] Pazos-Perez, N.; Pazos, E.; Catala, C.; Mir-Simon, B.; Gomez-de Pedro, S.; Sagales, J.; Villanueva, C.; Vila, J.; Soriano, A.; Garcia de Abajo, F. J.; Alvarez-Puebla, R. A. Ultrasensitive multiplex optical quantification of bacteria in large samples of biofluids. *Sci Rep* 2016, 6, 29014. doi:10.1038/srep29014.
- [26] Rivera-Betancourt O. E.; Karls, R.; Grosse-Siestrup, B.; Helms, S.; Quinn, F.; Dluhy, R. A. Identification of mycobacteria based on spectroscopic analyses of mycolic and acid profiles. *Analyst* 2013, 138, 6774. doi:10.1039/c3an01157g.
- [27] Henderson, K. C.; Sheppard, E. S.; Rivera-Betancourt O. E.; Choi, J.-Y.; Dluhy, R.A.; Thurman, K. A.; Winchell, J., M.; Krause, D. C. The multivariate detection limit for *Mycoplasma pneumoniae* as determined by nanorod array-surface enhanced Raman spectroscopy and comparison with limit of detection by qPCR. *Analyst* 2014, 24, 139, 6426–6434. doi:10.1039/c4an01141d.
- [28] Jin, H.; Wang, J.; Jin, S.; Jiang, L.; Zou, Y. Raman spectroscopy of potential bio-hazards commonly found in bio-aerosols. *Spectrochim Acta A Mol Biomol Spectrosc.* 2020, 243, 118753. doi:10.1016/j.saa.2020.118753.
- [29] Choi, J.; Lee, J.; Jung, J. H. Fully integrated optofluidic SERS platform for real-time and continuous characterization of airborne microorganisms. *Biosens Bioelectron.* 2020, 169, 112611. doi:10.1016/j.bios.2020.112611.
- [30] Park, K. J.; Wu, C.; Mercer-Smith, A.; Dodson, R. A.; Moersch, T. L.; Koonath, P. Raman system for sensitive and selective identification of volatile organic compounds. *Sens Act B: Chemical*, 2015; 220, 491–499. doi:10.1039/D0AY00180E.

- [31] Khan, Z. A.; Siddiqui, M. F.; Park, S. Current and Emerging Methods of Antibiotic Susceptibility Testing. *Diagnostics* 2019, 9, 49. doi:10.3390/diagnostics9020049.
- [32] Humphries, R. M.; Kircher, S.; Ferrell, A.; Krause, K. M.; Malherbe, R.; Hsiung, A.; Burnham, C.-A. D. The continued value of disk diffusion for assessing antimicrobial susceptibility in clinical laboratories: report from the Clinical and Laboratory Standards Institute Methods Development and Standardization Working Group. *J Clin Microbiol.* 2018, 56, e00437–18. doi:10.1128/JCM.00437-18.
- [33] Rodrigues, C.; Sousa, C.; Lopes, J. A.; Novais, Â.; Peixe, L. A frontline on *Klebsiella pneumoniae* capsular polysaccharide knowledge: Fourier transform infrared spectroscopy as an accurate and fast typing tool. *mSystems* 2020, 5, e00386–19. doi:10.1128/mSystems.00386-19.
- [34] Morais, I. M. C.; Cordeiro, A. L.; Teixeira, G. S.; Domingues, V. S.; Nardi, R. M. D.; Monteiro, A. S.; Alves, R. J.; Siqueira, E. P. Santos V. L. Biological and physicochemical properties of biosurfactants produced by *Lactobacillus jensenii* P6A and *Lactobacillus gasseri* P65. *Microb Cell Fact.* 2017, 16, 155. doi: 10.1186/s12934-017-0769-7.
- [35] Zimmermann, S.; Burckhardt, I. Development and Application of MALDI-TOF for Detection of Resistance Mechanisms. In MALDI-TOF and Tandem MS for Clinical Microbiology. Shah, H. N.; Saheer, E. G. Eds. John Wiley & Sons; Hoboken, NJ, USA, 2017; pp. 231–248.
- [36] Liu, C. -Y.; Han, Y. -Y.; Shih, P. -H.; Lian, W. -N.; Wang, H. -H.; Lin, C. -H.; Hsueh, P. -R.; Wang, J. -K.; Wang, Y. -L. Rapid bacterial antibiotic susceptibility test based on simple surface-enhanced Raman spectroscopic biomarkers. *Sci Rep.* 2016; 6. doi:10.1038/srep23375.
- [37] Schröder, U.C.; Beleites, C.; Assmann, C.; Glaser, U.; Hübner, U.; Pfister, W.; Fritzsche, W.; Popp, J.; Neugebauer, U. Detection of vancomycin resistances in enterococci within 3 K hours. *Sci. Rep.* 2015, 5, 8217. doi:10.1038/srep0821.
- [38] Dekter, H. E.; Orelia, C. C.; Morsink, M. C.; Tektas, S.; Vis, B.; te Witt, R.; van Leeuwen, W. B. Antimicrobial susceptibility testing of Gram-positive and -negative bacterial isolates directly from spiked blood culture media with Raman spectroscopy. *Eur J Clin Microbiol* 2017, 36, 81. doi:10.1007/s10096-016-2773-y.
- [39] Schröder, U. C.; Kirchhoff, J.; Hübner, U.; Mayer, G.; Glaser, U.; Henkel, T; Pfister, W.; Fritzsche, W.; Popp J.; Neugebauer, U. On-chip spectroscopic assessment of microbial susceptibility to antibiotics within 3.5 hours. *J Biophotonics* 2017, 10, 1547–1557. doi:10.1002/jbio.201600316.

- [40] Ho, C. S.; Jean, N.; Hogan, C. A.; Blackmon, L.; Jeffrey, S. S.; Holodniy, M.; Banaei, N.; Saleh, A. A. E.; Ermon, S.; Dionne, J. Rapid identification of pathogenic bacteria using Raman spectroscopy and deep learning. *Nat Commun.* 2019, 10, 4927. doi:10.1038/s41467-019-12898-9.
- [41] Bauer, D.; Wieland, K.; Qiu, L.; Neumann-Cip, A. C.; Magistro, G.; Stief, C.; Wieser, A.; Haisch, C. Heteroresistant Bacteria Detected by an Extended Raman-Based Antibiotic Susceptibility Test. *Anal Chem.* 2020, 92, 8722–8731. doi:10.1021/acs.analchem.9b05387.
- [42] Götz, T.; Dahms, M.; Kirchhoff, J.; Beleites, C.; Glaser, U.; Bohnert, J. A.; Pletz, M. W.; Popp, J.; Schlattmann, P.; Neugebauer, U. Automated and rapid identification of multidrug resistant *Escherichia coli* against the lead drugs of acylureidopenicillins, cephalosporins, and fluoroquinolones using specific Raman marker bands. *J Biophotonics.* 2020, 13, e202000149. doi:10.1002/jbio.202000149.
- [43] Centers for Disease Control and Prevention. Burden of Fungal Diseases in the United States. <https://www.cdc.gov/fungal/cdc-and-fungal/burden.html> (accessed April 21, 2021).
- [44] da Matta, D. A.; Souza, A. C. R.; Colombo, A. L. Revisiting Species Distribution and Antifungal Susceptibility of *Candida* Bloodstream Isolates from Latin American Medical Centers. *J Fungi* 2017, 3, 24. doi:10.3390/jof3020024.
- [45] Geddes-McAlister, J.; Shapiro, R. S. New pathogens, new tricks: emerging, drug-resistant fungal pathogens and future prospects for antifungal therapeutics. *Ann NY Acad Sci.* 2019, 1435, 57–78. doi:10.1111/nyas.13739.
- [46] Sekyere, J. O.; Asante, J. Emerging mechanisms of antimicrobial resistance in bacteria and fungi: advances in the era of genomics. *Future Microbiol.* 2018,13:241–262. doi: 10.2217/fmb-2017-0172.
- [47] Consortium OPATHY, Gabaldón, T. Recent trends in molecular diagnostics of yeast infections: from PCR to NGS. *FEMS Microbiol Rev.* 2019, 43, 517–547. doi:10.1093/femsre/fuz015.
- [48] Wohlmeister, D.; Vianna, D. R. B.; Helfer, V. E.; Calil, L. N.; Buffon, A.; Fuentesfria, A. M.; Corbellini, V. A.; Pilger, D. A. Differentiation of *Candida albicans*, *Candida glabrata*, and *Candida krusei* by FT-IR and chemometrics by CHROMagar™ *Candida*. *J Microbiol Methods* 2017, 141, 121–125. doi:10.1016/j.mimet.2017.08.013.
- [49] Colabella, C.; Corte, L.; Roscini, L.; Shapaval, V.; Kohler, A.; Tafintseva, V., Tascini, C.; Gardinali, G. Merging FT-IR and NGS for simultaneous phenotypic and genotypic identification of pathogenic *Candida* species. *PLoS ONE* 2017, 12, e0188104. doi: 10.1371/journal.pone.0188104.

- [50] Potocki, L.; Depciuch, J.; Kuna, E.; Worek, M.; Lewinska, A.; Wnuk, M. FTIR and Raman Spectroscopy-Based Biochemical Profiling Reflects Genomic Diversity of Clinical Candida Isolates That May Be Useful for Diagnosis and Targeted Therapy of Candidiasis. *Int J Mol Sci.* 2019, 20, 988. doi:10.3390/ijms20040988.
- [51] Tien, N.; Lin, T.H.; Hung, Z.C.; Lin, H. S.; Wang, I. K.; Chen, H. C.; Chang, C. T. Diagnosis of Bacterial Pathogens in the Urine of Urinary-Tract-Infection Patients Using Surface-Enhanced Raman Spectroscopy. *Molecules* 2018, 23, 3374. doi:10.3390/molecules23123374.
- [52] Ayala, O. D.; Doster, R. S.; Manning, S. D.; O'Brien, C. M.; Aronoff, D. M.; Gaddy, J. A.; Mahadevan-Jansen, A. Raman microspectroscopy differentiates perinatal pathogens on ex vivo infected human fetal membrane tissues. *J Biophotonics* 2019, 12, e201800449. doi:10.1002/jbio.201800449.
- [53] Kourkoumelis, N.; Gaitanis, G.; Velegraki, A.; Bassukas, I. D. Nail Raman spectroscopy: A promising method for the diagnosis of onychomycosis. An ex vivo pilot study. *Medical Mycology* 2018; 56, 551–558. doi:10.1093/mmy/myx078.
- [54] Gherman, A. M. R.; Dina, N. E.; Chiş, V.; Wieser, A.; Haisch, C. Yeast cell wall - Silver nanoparticles interaction: A synergistic approach between surface-enhanced Raman scattering and computational spectroscopy tools. *Spectrochim Acta A Mol Biomol Spectrosc.* 2019, 222, 117223. doi:10.1016/j.saa.2019.117223.
- [55] Ditta, A.; Nawaz, H.; Mahmood, T.; Majeed, M. I.; Tahir, M.; Rashid, N.; Muddassar, M.; Al-Saadi, A. A. Byrne HJ. Principal components analysis of Raman spectral data for screening of Hepatitis C infection. *Spectrochim Acta A Mol Biomol Spectrosc.* 2019, 221, 117173. doi:10.1016/j.saa.2019.117173.
- [56] Yeh, Y.-T.; Gulino, K.; Zhang, Y.; Sabestien, A.; Chou T.-W.; Zhou, B.; Lin, Z.; Albert, I.; Lu H.; Swaminathan, V.; Ghedin, E.; Terrones, M. A rapid and label-free platform for virus capture and identification from clinical samples. *PNAS* 2020 117, 895–901; doi:10.1073/pnas.1910113117.
- [57] Gahlaut, S. K.; Savargaonkar, D.; Sharan, C.; Yadav, S.; Mishra, P.; Singh, J. P. SERS Platform for Dengue Diagnosis from Clinical Samples Employing a Hand Held Raman Spectrometer. *Anal. Chem.* 2020, 92, 2527–2534. doi: 10.1021/acs.analchem.9b04129.
- [58] Yadav, S.; Senapati, S.; Desai, D.; Gahlaut, S.; Kulkarni, S.; Singh, J. P. Portable and sensitive Ag nanorods based SERS platform for rapid HIV-1 detection and tropism determination. *Colloids Surf B Biointerfaces.* 2021, 198, 111477. doi:10.1016/j.colsurfb.2020.111477.
- [59] Carlomagno, C.; Bertazioli, D.; Gualerzi, A.; Picciolini, S.; Banfi, P. I.; Lax, A.; Messina, E.; Navarro, J.; Bianchi, L.; Caronni, A.; Marengo, F.; Monteleone, S.; Arienti, C.; Bedoni, M. COVID-19 salivary Raman

- fingerprint: innovative approach for the detection of current and past SARS-CoV-2 infections. *Sci Rep* 2021, 11, 4943. doi:10.1038/s41598-021-84565-3.
- [60] Silva, L.; Rodrigues, C.; Lira, A.; Leão, M.; Mota, M.; Lopes, P.; Novais, Â.; Peixe, L. Fourier Transform Infrared (FT-IR) Spectroscopy Typing: A Real-Time Analysis of an Outbreak by Carbapenem-Resistant *Klebsiella pneumoniae*. *Eur J Clin Microbiol Infect Dis* 2020, 39, 2471–2475. doi:10.1007/s10096-020-03956-y.
- [61] Procházka, M. Surface-enhanced Raman spectroscopy. In *Biological and medical physics, biomedical engineering*. Springer International Publishing, Switzerland, 2016; pp 1–221.
- [62] Kögler, M.; Paul, A.; Anane, E.; Birkholz, M.; Bunker, A.; Viitala, T.; Maiwald, M.; Junne, S; Neubauer, P. Comparison of time-gated surface-enhanced raman spectroscopy (TG-SERS) and classical SERS based monitoring of *Escherichia coli* cultivation samples. *Biotechnol prog.* 2018, 34, 1533–1542. doi:10.1002/btpr.2665.
- [63] Kögler, M.; Itkonen, J.; Viitala, T.; Casteleijn, M. G. Assessment of recombinant protein production in *E. coli* with Time-Gated Surface Enhanced Raman Spectroscopy (TG-SERS). *Sci Rep.* 2020, 10, 1–11. doi:10.1038/s41598-020-59091-3.
- [64] Du, Z.; Qi, Y.; He, J.; Zhong, D.; Zhou, M. Recent advances in applications of nanoparticles in SERS in vivo imaging. *Wiley Interdiscip Rev Nanomed Nanobiotechnol.* 2021, 13, e1672. doi:10.1002/wnan.1672.
- [65] Kubryk, P.; Niessner, R.; Ivleva, N. P. The origin of the band at around 730 cm<sup>-1</sup> in the SERS spectra of bacteria: a stable isotope approach. *Analyst* 2016, 141, 2874–2878. doi:10.1039/c6an00306k.
- [66] Premasiri W. R.; Lemler, P.; Chen, Y.; Gebregziabher, Y.; Ziegler, L. A. SERS Analysis of Bacteria, Human Blood, and Cancer Cells: a Metabolomic and Diagnostic Tool. In *Frontiers of Surface-Enhanced Raman Scattering: Single Nanoparticles and Single Cells*; Ozaki, Y.; Kneipp, K.; Aroca, R. Eds. John Wiley & Sons, Ltd; Hoboken, New Jersey, USA, 2014; pp. 257–283.
- [67] Fargašová, A.; Balzerová, A.; Pucek, R.; Sedláková, M. H.; Bogdanová, K.; Gallo, J.; Kolář, M.; Ranc, V.; Zbořil, R. Detection of Prosthetic Joint Infection Based on Magnetically Assisted Surface Enhanced Raman Spectroscopy. *Anal Chem.* 2017, 89, 6598–6607. doi: 10.1021/acs.analchem.7b00759.
- [68] Bibikova, O.; Haas, J.; López-Lorente, A. I.; Popov, A.; Kinnunen, M.; Meglinski, I.; Mizaikoff, B. Towards enhanced optical sensor performance: SEIRA and SERS with plasmonic nanostars. *Analyst*, 2017, 142, 951–958. doi:10.1039/C6AN02596J.

- [69] Orelia, C. C.; Beiboer, S. H. W.; Morsink, M. C.; Tektas, S.; Dekter, H. E. van Leeuwen, W. B. Comparison of Raman spectroscopy and two molecular diagnostic methods for *Burkholderia cepacia* complex species identification. *J Microbiol Methods* 2014, 107, 126–132. doi:10.1016/j.mimet.2014.10.002.
- [70] Tsalik, E. L.; Lo, Y.; Hudson, L., L.; Chu, V. H.; Himme., T.; Limkakeng, A. T.; et al. Potential Cost-effectiveness of Early Identification of Hospital-acquired Infection in Critically Ill Patients. *Ann of Amer Thor Soc* 2015; 13: 401–413. doi:10.1513/AnnalsATS.201504-205OC.
- [71] Hu, J.; Wan, F.; Wang, P.; Ge, H.; Chen, W. Application of frequency-locking cavity-enhanced spectroscopy for highly sensitive gas sensing: a review. *Appl Spectr Rev.* 2021. doi:10.1080/05704928.2021.1894438.
- [72] Wang, C.; Sahay, P. Breath analysis using laser spectroscopic techniques: breath biomarkers, spectral fingerprints, and detection limits. *Sensors* 2009, 9, 8230–8262. doi:10.3390/s91008230.
- [73] Selvaraj, R.; Vasa, N. J. Nagendra SMS, Mizaikoff B. Advances in Mid-Infrared Spectroscopy-Based Sensing Techniques for Exhaled Breath Diagnostics. *Molecules* 2020, 25, 2227. doi:10.3390/molecules25092227.
- [74] Ahmed, W. M.; Lawal, O.; Nijsen, T.M.; Goodacre, R.; Fowler, S. J. Exhaled Volatile Organic Compounds of Infection: A Systematic Review. *ACS Infect Dis.* 2017, 3, 695–710. doi:10.1021/acsinfecdis.7b00088.
- [75] Magdy, C.; Issam, F.; Amir, P. Adel, S.; ElGohary, S. COVID-19 detection using SERS technique. *MOJ App Bio Biomech.* 2020, 4, 86–91. doi:10.15406/mojabb.2020.04.00141.
- [76] World Health Organization. Ten threats to global health in 2019. <https://www.who.int/news-room/spotlight/ten-threats-to-global-health-in-2019> (accessed March 31, 2021).
- [77] Centers for Disease Control and Prevention. Antibiotic/Antimicrobial Resistance (AR / AMR). <https://www.cdc.gov/drugresistance/index.html> (accessed March 31, 2021).
- [78] Burnham, C.-A. D.; Yarbrough, M. L. Best Practices for Detection of Bloodstream Infection. *J Appl Lab Med.* 2019, 3, 740–742. doi: 10.1373/jalm.2018.026260.
- [79] Neubrech, F.; Huck, C.; Weber, K.; Pucci, A.; Giessen, H. Surface-Enhanced Infrared Spectroscopy Using Resonant Nanoantennas. *Chem Rev.* 2017, 117, 5110–5145. doi:10.1021/acs.chemrev.6b00743.
- [80] Guyot, K.; Biran, V.; Doit, C.; Moissenet, D.;Guillard, T.; Brasme, L.; Courroux, C.; Maquelin, K.; van Leeuwen, W.; Vuthien, H.; Aujard, Y.; De Champs, C.; Bingen, E. Raman spectroscopic analysis of the clonal and horizontal spread of CTX-M-15-producing *Klebsiella pneumoniae* in a neonatal intensive care unit. *Eur J Clin Microbiol Infect Dis.* 2012, 31, 2827–2834. doi:10.1007/s10096-012-1636-4.
- [81] Willemse-Erix, D.; Bakker-Schut, T.; Slagboom-Bax, F.; Jachtenberg, J. W.; Lemmens-den Toom, N.; Papagiannitsis, C. C.; Kuntaman, K.; Puppels, G.; van Belkum, A.; Severin, J. A. Goessens W, Maquelin K.

- Rapid typing of extended-spectrum  $\beta$ -lactamase- and carbapenemase-producing *Escherichia coli* and *Klebsiella pneumoniae* isolates by use of SpectraCell RA. *J Clin Microbiol.* 2012, 50, 1370–1375. doi:10.1128/JCM.05423-11.
- [82] Avci, E.; Kaya, N.S.; Ucankus, G; Culha, M. Discrimination of urinary tract infection pathogens by means of their growth profiles using surface enhanced Raman scattering. *Anal Bioanal Chem.* 2015, 407, 8233–8241. doi:10.1007/s00216-015-8950-5.
- [83] Arend, N.; Pittner, A.; Ramoji, A.; Mondol, A. S.; Dahms, M.; Rüger, J.; Kurzai, O.; Schie, I. W.; Bauer, M.; Popp, J.; Neugebauer, U. Detection and Differentiation of Bacterial and Fungal Infection of Neutrophils from Peripheral Blood Using Raman Spectroscopy. *Anal Chem.* 2020, 92, 10560–10568. doi:10.1021/acs.analchem.0c01384.
- [84] Uusitalo, S.; Kögler, M.; Välimaa, A. L.; Popov, A.; Ryabchikov, Y.; Kontturi, V.; Hiltunen, J. Detection of *Listeria innocua* on roll-to-roll produced SERS substrates with gold nanoparticles. *RSC advances* 2016, 6, 62981–62989. doi:10.1039/C6RA08313G.

## Abbreviations

AMR	Antimicrobial resistance
ANN	Artificial neural network
AST	Antibiotic susceptibility testing
CW	Continuous wave
DNA	Deoxyribonucleic acid
FTIR	Fourier transform infrared
MIC	Minimum inhibitory concentrations
NHSA	National Healthcare Safety Network
PCA	Principal component analysis
POCT	Point-of-care testing
RNA	Ribonucleic acid
SEIRA	Surface-enhanced infrared absorption spectroscopy (SEIRAS)
SERS	Surface-enhanced Raman spectroscopy
TG	Time-gated
UTI	Urinary tract infection
VOC	Volatile organic compound

**Table 1.** Current clinical applications of Fourier transform infrared spectroscopy in microbiology.

Author (year)	Origin	Microbes	Wavenumber	Spectral preprocessing	Spectrometer	Chemometrics
Grunert et al. (2013) <sup>[17]</sup>	Clinical and veterinary isolates	<i>S. aureus</i>	4,000–500 cm <sup>-1</sup>	Savitzky-Golay filter, vector normalization	Tensor 27 in transmission mode	HCA, PCA, ANN
AlRabiah et al. (2014) <sup>[21]</sup>	Urine isolates	<i>E. coli</i>	4,000–600 cm <sup>-1</sup> at 4 cm <sup>-1</sup> resolution	NR	Equinox 55 in transmission mode	PCA, DFA, procrustes analysis, PCoA
Nyarko et al. (2014) <sup>[15]</sup>	Clinical and food isolates	<i>L. monocytogenes</i>	4,000–400 cm <sup>-1</sup>	Normalization and baseline correction	Tensor 27 in reflectance mode	CVA, LDA
Colabella et al. (2017) <sup>[49]</sup>	Blood isolates	<i>C. albicans</i> , <i>C. parapsilosis</i> , <i>C. glabrata</i> , <i>C. tropicalis</i>	4,000–400 cm <sup>-1</sup> at 4 cm <sup>-1</sup> resolution	Savitzky-Golay filter, EMSC	Tensor 27 with a transmission mode	CPCA, PLSR, Mantel test, cross-validation
Morais et al. (2017) <sup>[34]</sup>	Vaginal isolates	<i>L. jensenii</i> , <i>L. gasseri</i>	4,000–650 cm <sup>-1</sup> at 4 cm <sup>-1</sup> resolution	NR	Spectrum-One™ with ATR	NR
Wohlmeister et al. 2017 <sup>[48]</sup>	Vaginal isolates	<i>C. albicans</i> , <i>C. albicans</i> , <i>C. glabrata</i> , <i>C. glabrata</i> , <i>C. glabrata</i> , <i>C. krusei</i>	4,000–450 cm <sup>-1</sup> at 4 cm <sup>-1</sup> resolution	Normalization and baseline correction	Spectrum 400 with diffuse reflectance	PCA, SIMCA
Lasch et al. (2018) <sup>[14]</sup>	RKI sample and <i>Burkholderia</i> species-level sets	<i>Bacillus</i> , <i>Enterococcus</i> , <i>Staphylococcus</i> , <i>Citrobacter</i> , <i>Pseudomonas</i> , <i>Escherichia</i>	3,800–900 cm <sup>-1</sup> at 8 cm <sup>-1</sup> resolution	ROI	Agilent 670 in transmission mode	ANN
Martak et al. (2019) <sup>[16]</sup>	Clinical isolates	<i>P. aeruginosa</i> , <i>K. pneumoniae</i> , <i>E. cloacae</i> , <i>A. baumannii</i>	4,000–400 cm <sup>-1</sup>	Vector normalization, 2 <sup>nd</sup> derivative	IR Biotyper in transmission mode	HCA

Potocki et al. (2019) <sup>[50]</sup>	BAL, sputum, pharynx, wound, urine, and vaginal isolates	<i>C. albicans</i> , <i>C. tropicalis</i> , <i>C. glabrata</i>	4,000–400 cm <sup>-1</sup> at 2 cm <sup>-1</sup> resolution	Normalization and baseline correction	Vertex 70v with ATR	PCA, HCA
Vogt et al. (2019) <sup>[18]</sup>	Anal and pharyngeal isolates	<i>E. hormaechei</i> , <i>E. asburiae</i> , <i>E. ludwigii</i> , <i>E. bugandensis</i>	1,300–800 cm <sup>-1</sup>	Vector normalization, 2 <sup>nd</sup> derivative	IR Biotyper with default analysis	PCA, ANN
Guliev et al. (2020) <sup>[13]</sup>	Clinical isolates	<i>S. capitis</i> , <i>S. epidermidis</i> , <i>S. hemolyticus</i> , <i>S. hominis</i> , <i>S. simulans</i> , <i>S. warneri</i> , <i>S. sciuri</i>	4,000–600 cm <sup>-1</sup> at 4 cm <sup>-1</sup> resolution	AVC	Spectrum Two™ in transmission mode	PCA, LDA, AUC, TPR, FPR
Rodrigues et al. (2020) <sup>[33]</sup>	Clinical isolates	<i>K. pneumoniae</i>	4,000–600 cm <sup>-1</sup> at 4 cm <sup>-1</sup> resolution	Savitzky-Golay filter, SNV	Spectrum BX with ATR	PCA, HCA, PLSDA, SID
Silva et al. (2020) <sup>[60]</sup>	KPC-3-producing <i>K. pneumoniae</i> isolates	<i>K. pneumoniae</i>	1200–900 cm <sup>-1</sup>	NR	IR Biotyper with ATR	PCA, PLSDA

Abbreviations: ANN = artificial neural network; ATR = attenuated total reflectance mode; AUC = area under the ROC curve; AVC = atmospheric vapor compensation; BAL = bronchoalveolar lavage; CPCA = consensus principal component analysis; CVA = canonical variate analysis; DFA = discriminant function analysis; EMSC = extended multiplicative signal correction; FPR = false positive rate; HCA = hierarchical cluster analysis; LDA = linear discriminant analysis; NR = not reported; PCA = principal component analysis; PCoA = principal coordinate analysis; PLSDA = partial least-squares discriminant analysis; PLSR = partial least-squares regression; ROI = region of interest; SID = Simpson's index of diversity; TPR = true positive rate; SIMCA = soft independent modeling by class analog; SNV = standard normal variate.

**Table 2.** The diagnostic accuracy of FTIR spectroscopy in microbiology.

Author (year)	Origin	Microbes	Advantages	Disadvantages
Grunert et al. (2013) <sup>[17]</sup>	Clinical and veterinary isolates	<i>S. aureus</i>	Accurate (96.7–98.2%), low cost, fast (1 day for the growth of bacteria, <5 min for sample preparation per strain), little sample preparation, data analysis automated, externally validated	
AlRabiah et al. (2014) <sup>[21]</sup>	Urine	<i>E. coli</i>	Accurate (PE: 0.53–0.93)	Lack of correlation with metabolic test
Nyarko et al. (2014) <sup>[15]</sup>	Clinical and food isolates	<i>L. monocytogenes</i>	Accurate (100%), fast (sample collection: 5 min; spectral processing: 60min; incubation: 14 hours), and potentially less expensive	
Colabella et al. (2017) <sup>[49]</sup>	Blood	<i>C. albicans</i> , <i>C. parapsilosis</i> , <i>C. glabrata</i> , <i>C. tropicalis</i>	Accurate (93.1–97.4%) for <i>C. albicans</i> and <i>C. glabrata</i>	Limited accuracy (80–82%) for <i>C. parapsilosis</i> and <i>C. tropicalis</i> , lack of spectral libraries
Morais et al. (2017) <sup>[34]</sup>	Vaginal isolates	<i>L. jensenii</i> , <i>L. gasseri</i>	Kinetics information, AST	
Wohlmeister et al. 2017 <sup>[48]</sup>	Vaginal isolates	<i>C. albicans</i> , <i>C. glabrata</i> , <i>C. krusei</i>	Accurate (93.4%), low cost, fast	Limited amount of spectrum replicates
Lasch et al. (2018) <sup>[14]</sup>	RKI sample and <i>Burkholderia</i> species-level sets	<i>Bacillus</i> , <i>Enterococcus</i> , <i>Staphylococcus</i> , <i>Citrobacter</i> , <i>Pseudomonas</i> , <i>Escherichia</i>	Accurate (75%), low cost, fast, relatively short cultivation time	Proof-of-principle study, lack of standardized culture conditions, sample preparations, and spectral libraries
Martak et al. (2019) <sup>[16]</sup>	Clinical isolates	<i>P. aeruginosa</i> , <i>K. pneumoniae</i> , <i>E. cloacae</i> , <i>A. baumannii</i>	Accurate (AR 0.76–1.00, AW 0.88–1.00), reproducible, fast	Lack of standardized culture conditions and sample preparations
Potocki et al. (2019) <sup>[50]</sup>	BAL, sputum, pharynx, wound, urine, and vaginal isolates	<i>C. albicans</i> , <i>C. tropicalis</i> , <i>C. glabrata</i>	Accurate (74–97.4%), fast	Limited differentiation ability

Vogt et al. (2019) <sup>[18]</sup>	Anal and pharyngeal isolates	<i>E. hormaechei</i> , <i>E. asburiae</i> , <i>E. ludwigii</i> , <i>E. bugandensis</i>	Concordant (ARI 0.80–0.82), low cost, fast (3h)	
Guliev et al. (2020) <sup>[13]</sup>	Clinical isolates	<i>S. capitis</i> , <i>S. epidermidis</i> , <i>S. hemolyticus</i> , <i>S. hominis</i> , <i>S. simulans</i> , <i>S. warneri</i> , <i>S. sciuri</i>	Sensitive (100%), specificity (98%), externally validated	Lack of reproducibility due to the lack of standardized culture conditions, sample preparations, and spectral libraries
Rodrigues et al. (2020) <sup>[33]</sup>	Clinical isolates	<i>K. pneumoniae</i>	Accurate (SID: 0.93; 95% CI: 0.92–0.95), reproducible, low cost, rapid AST	Lack of standardized culture conditions, sample preparations, and automation of data analysis
Silva et al. (2020) <sup>[60]</sup>	KPC-3-producing <i>K. pneumoniae</i> isolates	<i>K. pneumoniae</i>	Accurate, low cost, fast, no sample extraction	
AR = adjusted Rand; ARI = adjusted Rand index; AST = antibiotic susceptibility testing; AW = adjusted Wallace coefficient; BAL = bronchoalveolar lavage; CI= confidence interval; NR = not reported; PE = procruster error; SID = Simpson's index of diversity				

**Table 3.** Current clinical applications of Raman spectroscopy in microbiology.

Author (year)	Origin	Microbes	Spectroscopic parameters	Spectral preprocessing	Spectrometer	Chemometrics
Guyot et al. (2012) <sup>[80]</sup>	Clinical and environmental isolates	<i>K. pneumoniae</i>	220 mW of laser light (785 nm) for 1 s	NR	NR	PCC, UPGM
Willemsse-Erix et al. (2012) <sup>[81]</sup>	Urine (52%) and wound swab isolates	<i>E. coli</i> , <i>K. pneumoniae</i>	220 mW of laser light (785 nm) for 1 s	NR	SpectraCell RA	PCC
Rivera-Betancourt et al. (2013) <sup>[26]</sup>	Clinical isolates	<i>Mycobacterium</i> species	15 mW of laser light (785 nm) in 1,700–700 $\text{cm}^{-1}$ for 10 s	Savitzky-Golay filter	Unity Inova 500	PCA, HCA, PLS-DA
Schröder et al. (2013) <sup>[23]</sup>	Urine isolates	<i>E. coli</i> , <i>E. faecalis</i>	15 mW of laser light (532 nm) in 1,750–600 $\text{cm}^{-1}$	NR	WITec Alpha300 R	PCA, LDA
Henderson et al. (2014) <sup>[27]</sup>	Respiratory secretions	<i>M. pneumoniae</i>	28 mW of laser light (785 nm) in 1,800–400 $\text{cm}^{-1}$ for 10 s	SNR	WiRE	PCA, HCA, PLS-DA
Avci et al. (2015) <sup>[82]</sup>	Clinical isolates	<i>E. coli</i> , <i>E. faecalis</i> , <i>S. aureus</i> , <i>S. saprophyticus</i> , <i>K. pneumoniae</i>	0.3–3 mW of diode laser light (830 nm) in 520 $\text{cm}^{-1}$ for 10 s	Cubic spline interpolation	Renishaw InVia	PCA
Park et al. (2015) <sup>[30]</sup>	Gas isolates	<i>P. aeruginosa</i> , <i>S. aureus</i> , <i>E. coli</i>	250 mW of laser light (830 nm) in 1,000–500 $\text{cm}^{-1}$ for 30 s	Removal background and suppress noise, 2D correlation analysis	Dimension-P2™	PCA
Schröder et al. (2015) <sup>[37]</sup>	Clinical isolates	<i>E. faecalis</i> , <i>E. faecium</i>	15 mW of laser light (532 nm) in 3,100–2,800 and 1,800–600 $\text{cm}^{-1}$ for 1 s at 10 $\text{cm}^{-1}$ resolution	NR	CRM 300 WITec	PLS, LDA

Liu et al. (2016) <sup>[36]</sup>	Clinical isolates	<i>S. aureus</i> , <i>E. coli</i> , <i>A. baumannii</i> , <i>K. pneumoniae</i>	105 mW/cm <sup>2</sup> of laser light (632.8 nm) for 1–3 s at sub-10 nm resolution	NR	HR800	NR
Pazos-Perez et al. (2016) <sup>[25]</sup>	Serum and blood isolates	<i>E. coli</i> , <i>P. aeruginosa</i> , <i>S. aureus</i> , <i>S. agalactiae</i>	300 mW of laser light (785 nm) for 100 ms at high resolution (1200 g cm <sup>-1</sup> )	NR	Lambda 19	PCA, CLS
Fargašová et al. (2017) <sup>[67]</sup>	Knee joint fluid isolates	<i>S. aureus</i> , <i>S. pyogenes</i>	5.0 mW of laser light (633 nm) in 1,800–400 cm <sup>-1</sup> for 0.5 s	NR	Nicolet iS5	MA-SERS
DeJong et al. (2017) <sup>[22]</sup>	Blood and urine isolates	<i>E. coli</i> , <i>E. cloacae</i> , <i>E. marcescens</i>	NR	SNR	Hamamatsu c12710	NR
Dekter et al. (2017) <sup>[38]</sup>	Blood isolates	<i>E. faecalis</i> , <i>E. faecium</i> , <i>S. aureus</i> , <i>E. cloacae</i> , <i>E. coli</i> , <i>K. pneumoniae</i> , <i>P. aeruginosa</i> , <i>S. marcescens</i>	45–50 mW of laser light (785 nm) in 3,100–150 cm <sup>-1</sup> for 10 s at 4 cm <sup>-1</sup> resolution	Calibration and standardization	A MoiD system	HCA, UPGMA
Schröder et al. (2017) <sup>[39]</sup>	Urine isolates	<i>E. coli</i>	36 mW of laser light (532 nm) in 3,120–1,800 cm <sup>-1</sup> for 2 s	NR	CRM 300 WITec	PLS, LDA
Kourkoumelis et al. (2018) <sup>[53]</sup>	Nail isolates	<i>C. parapsilosis</i> , <i>C. glabrata</i> , <i>C. albicans</i> , <i>T. rubrum</i>	30 mW of laser light (785 nm) in 3,200–200 cm <sup>-1</sup> for 5 s at ~4.5 cm <sup>-1</sup> resolution	Savitzky-Golay filter, SNV	NR	PCA, SIMCA, PLS-DA
Tien et al. (2018) <sup>[51]</sup>	Urine isolates	<i>E. coli</i> , <i>S. aureus</i> , <i>E. faecalis</i>	20 mW of laser light (785 nm) in 2000–400 cm <sup>-1</sup> for 5 s	NR	NR	PCA

Ayala et al. (2019) <sup>[52]</sup>	Fetal membrane tissue isolates	<i>S. agalactiae</i> , <i>E. coli</i> , <i>S. aureus</i>	12 mW of laser light (830 nm) in 1,700–800 $\text{cm}^{-1}$ for 15 s at $\sim 1 \text{ cm}^{-1}$ resolution	Background subtraction and noise smoothing	Renishaw InVia	PCA, SVD, HCA, SMLR
Ho et al. (2019) <sup>[40]</sup>	Blood, urine, and sputum isolates	<i>P. aeruginosa</i> , <i>S. aureus</i> , <i>S. epidermitis</i> , <i>S. lugotunensis</i> , <i>S. pneumoniae</i> , <i>S. sanguinis</i> , <i>S. marcescens</i> , <i>S. enterica</i> , <i>E. faecalis</i> , <i>E. faecium</i> , <i>E. coli</i> , <i>E. cloacae</i> , <i>K. pneumoniae</i> , <i>K. aerogenes</i> , <i>C. albicans</i> , <i>C. glabrata</i>	13.2 mW of laser light (633 nm) in 1,792–382 $\text{cm}^{-1}$	NR	NR	CNN, SMV
Gherman et al. (2019) <sup>[54]</sup>	Clinical isolates	<i>C. albicans</i> , <i>C. glabrata</i> , <i>C. parapsilosis</i>	7 mW of laser light (7514 nm) in 1,800–400 $\text{cm}^{-1}$ for 10 s	Normalization and baseline correction	Renishaw 2000	PCA, LDA
Potocki et al. (2019) <sup>[49]</sup>	BAL, sputum, pharynx, wound, urine, and vaginal isolates	<i>C. albicans</i> , <i>C. tropicalis</i> , <i>C. glabarata</i>	1.5 W of laser light (1064 nm) in 3,700–150 $\text{cm}^{-1}$ at 8 $\text{m}^{-1}$ resolution	NR	Nicolet NXR 9650	PCA, HCA
Yeh et al. (2019) <sup>[56]</sup>	Clinical isolates	<i>Rhinovirus</i> , <i>influenza virus</i> , <i>parainfluenza viruses</i>	NR	NR	VIRRION platform	PCA, 3-fold cross-validation
Arend et al. (2020) <sup>[83]</sup>	Blood isolates	<i>S. aureus</i> , <i>E. coli</i> , <i>C. albicans</i>	35 mW of laser light (532 nm) for 1 s	NR	WITec Alpha300R	PCA, LDA

Bauer et al. (2020) <sup>[41]</sup>	Clinical isolates	<i>E. coli</i> , <i>E. faecalis</i> , <i>E. faecium</i>	10 mW of laser light (532 nm) in 3,120–1,800 cm <sup>-1</sup> for 3 s	Normalization of the background-subtracted spectra	WITec Alpha300 R	MLR, SVM
Choi et al. (2020) <sup>[29]</sup>	Sampled air	<i>S. epidermidis</i> , <i>M. luteus</i> , <i>E. hirae</i> , <i>B. subtilis</i> , <i>E. coli</i>	DPSS laser (785 nm)	NR	Optofluidic SERS platform	PCA
Gahlaut et al. (2020) <sup>[57]</sup>	Blood isolates	Dengue virus	50 mW of laser light (785 nm) in 2,000–250 cm <sup>-1</sup> at 60 s	NR	ASSURX	PCA
Götz et al. (2020) <sup>[42]</sup>	Urine isolates	<i>E. coli</i>	Laser light of 532 nm in 1,800–600 cm <sup>-1</sup> at 5 cm <sup>-1</sup> resolution	Normalization and baseline correction	CRM300	Normalized and weighted sum scores
Jin et al. (2020) <sup>[28]</sup>	Pollen, bacterial, and fungal isolates	<i>S. aureus</i> , <i>E. coli</i> , <i>C. albicans</i>	50 mW of laser light (532 nm) in 1,800–300 cm <sup>-1</sup> for 10 s	Savitzky-Golay filter	Horiba Labram HR Evolution	PCA, SMV
Carlomagno et al. (2021) <sup>[59]</sup>	Saliva isolates	SARS-CoV-2	512 mW of laser light (785 nm) in 1,600–400 cm <sup>-1</sup> at 0.8 cm <sup>-1</sup> resolution	Savitzky-Golay filter	Aramis	PCA, LDA, LOOCV
Yadav et al. (2021) <sup>[58]</sup>	Blood isolates	Human immune-deficiency virus	20 mW of laser light (785 nm) in 1,800–300 cm <sup>-1</sup> at 20–40 s	NR	ASSURX	PCA

Abbreviations: CLS = classical least squares; CNN= convolutional neural network; HCA = hierarchical cluster analysis; LDA = linear discriminant analysis; LOOCV = Leave-one-out cross validation; MA-SERS = magnetically assisted surface enhanced Raman spectroscopy; MLR = multiple linear regression; NR = not reported; PCA = principal component analysis; PCC = Pearson correlation coefficient; PCoA = principal coordinate analysis; PLS = partial least-squares; PLS-DA = partial least-squares discriminant analysis; SIMCA = soft independent modeling by class analog; SMLR = sparse multinomial logistic regression; SNR = signal-to-noise ratio; SNV = standard normal variate; SVD = singular value decomposition; SVM = support vector machine; UPGM = unweighted pair-group method with averages; UPGMA = unweighted pair group method with arithmetic mean.

**Table 4.** The diagnostic accuracy of Raman spectroscopy in microbiology.

Author (year)	Origin	Microbes	Advantages	Disadvantages
Guyot et al. (2012) <sup>[80]</sup>	Clinical and environmental isolates	<i>K. pneumoniae</i>	Good agreement	
Willemsse-Erix et al. (2012) <sup>[81]</sup>	Urine and wound swab isolates	<i>E. coli</i> , <i>K. pneumoniae</i>	Accurate (95–97%), sensitive (95%), specificity (83%), fast, easy-to-use	
Rivera-Betancourt et al. (2013) <sup>[26]</sup>	Clinical isolates	<i>Mycobacterium</i> species	Accurate (100%), sensitive (83–100%), specificity (80–100%), fast	
Schröder et al. (2013) <sup>[23]</sup>	Urine isolates	<i>E. coli</i> , <i>E. faecalis</i>	Very good agreement, fast, low cost, label free and easy to use, a short sample preparation time	Proof-of-principle study
Henderson et al. (2014) <sup>[27]</sup>	Respiratory secretions	<i>M. pneumoniae</i>	Sensitive (90–100%), fast, minimal sample preparation, clinically relevant concentrations	Complex clinical background
Avcı et al. (2015) <sup>[82]</sup>	Urine isolates	<i>E. coli</i> , <i>E. faecalis</i> , <i>S. aureus</i> , <i>S. saprophyticus</i> , <i>K. pneumoniae</i>	Highly reproducible, strong consistency, fast (13 min for spectral processing, 1 h for incubation), kinetics information	
Park et al. (2015) <sup>[30]</sup>	Gas isolates	<i>P. aeruginosa</i> , <i>S. aureus</i> , <i>E. coli</i>	Good agreement, sensitivity in the low-ppm range, kinetics information	Proof-of-principle study
Schröder et al. (2015) <sup>[37]</sup>	Clinical isolates	<i>E. faecalis</i> , <i>E. faecium</i> ,	Sensitive (87–93%), specificity (77–99%), rapid AST and MIC determination (spectral processing: 35 min),	Proof-of-principle study
Liu et al. (2016) <sup>[36]</sup>	Clinical isolates	<i>S. aureus</i> , <i>E. coli</i> , <i>A. baumannii</i> , <i>K. pneumoniae</i>	Good agreement, rapid AST and MIC determination (2 h for incubation)	Proof-of-principle study

Pazos-Perez et al. (2016) <sup>[25]</sup>	Serum and blood isolates	<i>E. coli</i> , <i>P. aeruginosa</i> , <i>S. aureus</i> , <i>S. agalactiae</i>	Fast, clinically relevant concentrations, kinetics information	Limited discrimination ability
Fargašová et al. (2017) <sup>[67]</sup>	Knee joint fluid isolates	<i>S. aureus</i> , <i>S. pyogenes</i>	Sensitive, low cost, fast, versatile, viability	Limited stability
DeJong et al. (2017) <sup>[22]</sup>	Blood and urine isolates	<i>E. coli</i> , <i>E. cloacae</i> , <i>S. marcescens</i>	Clinically relevant concentrations within 16 hours	Proof-of-principle study
Dekter et al. (2017) <sup>[38]</sup>	Blood isolates	<i>E. faecalis</i> , <i>E. faecium</i> , <i>S. aureus</i> , <i>E. cloacae</i> , <i>E. coli</i> , <i>K. pneumoniae</i> , <i>P. aeruginosa</i> , <i>S. marcescens</i>	High similarity (99.1%), low cost, rapid AST and MIC determination	Proof-of-principle study, limited concordance (65–100%), further optimization required
Schröder et al. (2017) <sup>[39]</sup>	Urine isolates	<i>E. coli</i>	Sensitive (>90%), rapid AST	Limited specificity (75%)
Kourkoumelis et al. (2018) <sup>[53]</sup>	Nail isolates	<i>C. parapsilosis</i> , <i>C. glabrata</i> , <i>C. albicans</i> , <i>T. rubrum</i>	Accurate (92.8–100%)	Lack of clinical translation
Tien et al. (2018) <sup>[51]</sup>	Urine isolates	<i>E. coli</i> , <i>S. aureus</i> , <i>E. faecalis</i>	High similarity (>95%), low cost, rapid AST and MIC determination	Lack of spectral libraries
Ayala et al. (2019) <sup>[52]</sup>	Fetal membrane tissue isolates	<i>S. agalactiae</i> , <i>E. coli</i> , <i>S. aureus</i>	Sensitive (100.0%), specificity (88.9%), fast	Lack of spectral libraries
Ho et al. (2019) <sup>[40]</sup>	Clinical isolates	<i>C. albicans</i> , <i>C. glabrata</i> , <i>C. parapsilosis</i>	Accurate (99.7±1.1%), rapid AST	Proof-of-principle study, lack of automated sample preparation and data acquisition processes
Gherman et al. (2019) <sup>[54]</sup>	Clinical isolates	<i>C. albicans</i> , <i>C. glabrata</i> , <i>C. parapsilosis</i>	Correctness (100%)	
Potocki et al. (2019) <sup>[49]</sup>	BAL, sputum, pharynx, wound, urine, and vaginal isolates	<i>C. albicans</i> , <i>C. tropicalis</i> , <i>C. glabrata</i>	Accurate (97–100%), easy-to-use, fast for azole susceptibility testing	Lack of spectral libraries
Yeh et al. (2019) <sup>[56]</sup>	Clinical isolates	<i>Rhinovirus</i> , <i>influenza virus</i> , <i>parainfluenza viruses</i>	Accurate (70–90%), specificity (90%), low cost, fast	
Arend et al. (2020) <sup>[83]</sup>	Blood isolates	<i>S. aureus</i> , <i>E. coli</i> , <i>C. albicans</i>	Accurate (90–92%), fast	Proof-of-principle study

Bauer et al. (2020) <sup>[41]</sup>	Clinical isolates	<i>E. coli</i> , <i>E. faecalis</i> , <i>E. faecium</i>	Good agreement, rapid AST and MIC determination (3.5 h), stable	Lack of clinical translation, viability
Choi et al. (2020) <sup>[29]</sup>	Sampled air	<i>S. epidermidis</i> , <i>M. luteus</i> , <i>E. hirae</i> , <i>B. subtilis</i> , <i>E. coli</i>	Efficient (98.2–99.4%), fast, clinically relevant concentrations	Lack of validation
Gahlaut et al. (2020) <sup>[57]</sup>	Blood isolates	Dengue virus	Rapid, portable, cost-effective technique for POCT with high sensitivity and reproducibility.	
Götz et al. (2020) <sup>[42]</sup>	Urine isolates	<i>E. coli</i>	Sensitive (76–100%), specificity (81–97%), fast for AST (<3 h), kinetics information	Proof-of-principle study
Jin et al. (2020) <sup>[28]</sup>	Pollen, bacterial, and fungal isolates	<i>S. aureus</i> , <i>E. coli</i> , <i>C. albicans</i>	Accurate (97.3%), fast (3–4 h for incubation)	
Carlomagno et al. (2021) <sup>[59]</sup>	Saliva isolates	SARS-CoV-2	Accurate (87.6%), sensitive (83.7%), specificity (92.2%), fast	
Yadav et al. (2021) <sup>[58]</sup>	Blood isolates	Human immunodeficiency virus	sensitive (85.2%), specificity (84.8 %)	
AUC = area under the curve; AST = antibiotic susceptibility testing; BAL = bronchoalveolar lavage; MIC = minimum inhibitory concentration; NR = not reported; POCT = point-of-care testing.				

## Figure captions

**Fig. 1.** A Fourier transform infrared spectrum of dried human serum, measured using the attenuated total reflectance (ATR) method.

**Fig. 2.** The Raman spectrum of human serum dried on a steel plate. A Raman microscope with an excitation wavelength of 785 nm was used for the measurement.

**Fig. 3.** Figure 3a exemplifies the differences and similarities of the CW-SERS (Ag NPs) spectra of *E. coli* and *S. aureus* at an identical concentration, using the identical confocal Raman spectroscopy microscope's set-up and settings. In Figure 3b, different set-ups are used, namely TG-SERS at  $\lambda_{\text{exc}} = 532$  nm pulsed laser excitation and CW-SERS at  $\lambda_{\text{exc}} = 785$  nm continuous laser excitation. Apart from differences due to the set-up (i.e., higher Raman sensitivity in the case of TG-SERS and the microorganisms used), one common characteristic for bacteria identification with SERS is the peak at around  $730\text{ cm}^{-1}$ , as can be seen in Figure 3. This peak often even shows the strongest intensity at low concentrations, and this can be assigned to adenine and may be used as marker of the presence of bacteria. Fig. 3b is reproduced with permission (Uusitalo et al., 2016).<sup>[84]</sup>

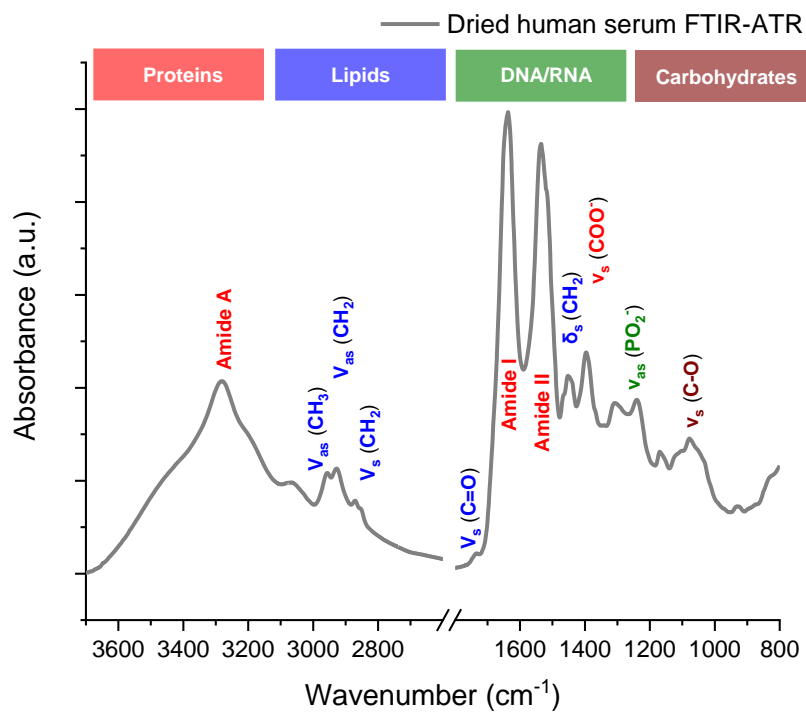


**Fig. 1.** A Fourier transform infrared spectrum of dried human serum, measured using the attenuated total reflectance (ATR) method.

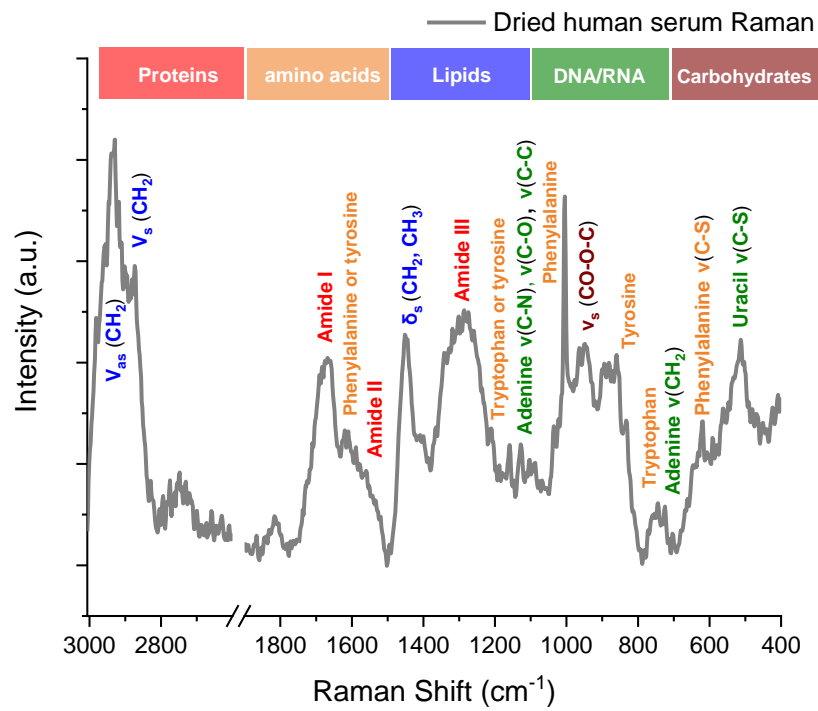


**Fig. 2.** The Raman spectrum of human serum dried on a steel plate. A Raman microscope with an excitation wavelength of 785 nm was used for the measurement.

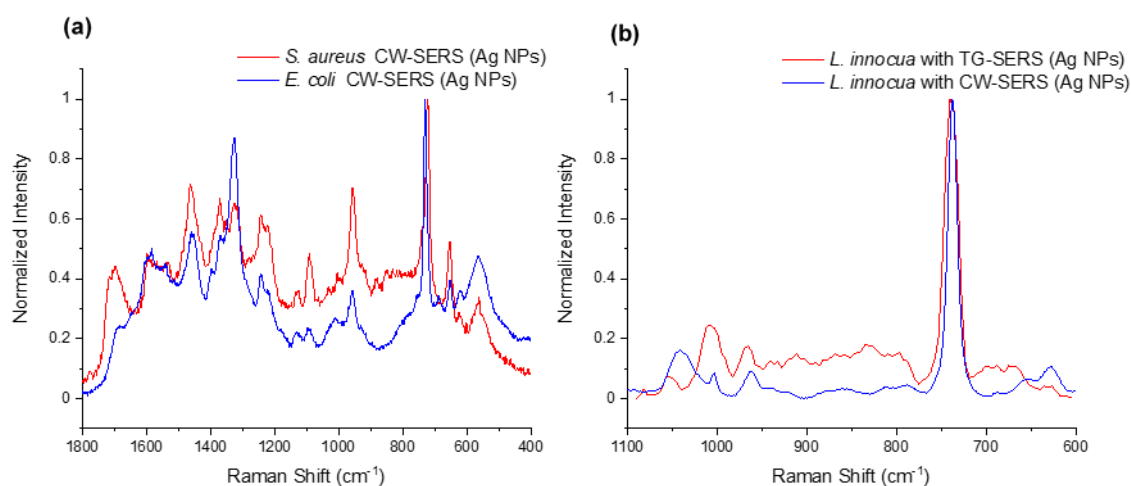


**Fig. 3.** Figure 3a exemplifies the differences and similarities of the CW-SERS (Ag NPs) spectra of *E. coli* and *S. aureus* at an identical concentration, using the identical confocal Raman spectroscopy microscope's set-up and settings. In Figure 3b, different set-ups are used, namely TG-SERS at  $\lambda_{\text{exc}} = 532$  nm pulsed laser excitation and CW-SERS at  $\lambda_{\text{exc}} = 785$  nm continuous laser excitation. Apart from differences due to the set-up (i.e., higher Raman sensitivity in the case of TG-SERS and the microorganisms used), one common characteristic for bacteria identification with SERS is the peak at around  $730\text{ cm}^{-1}$ , as can be seen in Figure 3. This peak often even shows the strongest intensity at low concentrations, and this can be assigned to adenine and may be used as marker of the presence of bacteria. Fig. 3b is reproduced with permission (Uusitalo et al., 2016).<sup>[84]</sup>